Bench-Scale Experiment of Dynamic Wireless Power Transfer System with Grid-Connected Photovoltaic and DC Bus Voltage Control

Nozomi MURAYAMA
Faculty of Science and Technology
Tokyo University of Science
Noda, Japan
murayama.nozomi23@gmail.com

Takehiro IMURA
Faculty of Science and Technology
Tokyo University of Science)
Noda, Japan

Yoichi HORI
Faculty of Science and Technology
Tokyo University of Science
Noda, Japan

***Abstract*—In recent years, the Dynamic Wireless Power Transfer (DWPT) system has been attracting attention as a promising solution to the problems that Electric Vehicles (EVs) face, such as long charging times and short cruising ranges. In this study, we propose a system that uses a grid-connected Photovoltaic (PV) as an energy source for DWPT. When the power generated by PV exceeds the amount needed for DWPT, the surplus power is fed back into the grid. Conversely, additional power is drawn from the grid if the PV power is insufficient, maintaining the DC bus voltage constant. In this way, a stable power supply to EVs, the power demand side, can be achieved. The effectiveness of the proposed system, which enables stable DWPT while performing maximum power point tracking (MPPT) control on the PV side and DC bus voltage control on the Grid side, was verified using circuit analysis software (MATLAB/Simulink) and a laboratory workable bench-scale experiment. The results indicated that the DC bus voltage remained within plus or minus 1% of the target value, regardless of fluctuations in PV power or changes in the coupling coefficient between transmitting and receiving coils. Additionally, the DWPT system achieved a maximum power transmission efficiency of approximately 88%, confirming the effectiveness of the proposed approach.**

Keywords—Dynamic Wireless Power Transfer, Photovoltaic, Electric Vehicles, MPPT, Grid-connected, DAB converter, DC bus, Bench-Scale Experiment

I. INTRODUCTION

Lately, there has been a shift from gasoline-powered vehicles to electric vehicles (EVs) powered by electricity. However, EVs have some problems: their cruising range is shorter than that of gasoline-powered vehicles, there are few recharging facilities, and recharging takes a long time. As a solution to these problems, Dynamic Wireless Power Transfer (DWPT) has been studied [1]-[4], which wirelessly transmits power from roadside facilities to EVs while in motion.

The DWPT system enhances the charging infrastructure and extends the cruising range without requiring an increase in the EV's battery capacity. Moreover, by utilizing photovoltaic (PV) energy, a renewable resource, as the power supply for the DWPT, it aims to further promote decarbonization.

This paper proposes a PV + DWPT system in which the power source of the DWPT is grid-connected photovoltaic power generation.

In [5], which examines a system integrating PV and DWPT, describes a mechanism where the power source is switched, resulting in the suspension of PV generation when DWPT is not in operation. To eliminate this waste of power, some studies have connected PV to the Grid or batteries to save the PV power [6][7]. In this paper, we connect a DAB converter, an isolated bidirectional DC/DC converter, to the DC grid, like the PV+DWPT system in [8], which I wrote previously.

When the PV is generating excess power, the excess power is returned to the DC grid, and when the PV is not generating enough power, the additional power is made up from the grid. In addition, a DAB converter is used to control the DC bus voltage to enable stable DWPT. Based on the simulation results in [8] and further simulation results, a bench-scale experiment, which is a scaled-down version of the actual experiment, was conducted to further the practical application of the proposed system.

In section II, the circuit configuration and control method of the proposed system are presented. In III, the methods of simulation and bench-scale experiments are presented, and in IV, the results of each are shown. Finally, section V presents the conclusion.

II. PROPOSED PV+DWPT SYSTEM

A. System Configuration

An image of the proposed system in this paper is shown in Fig. 1. As shown in Fig. 1, the PV panel and power system are connected to a common DC bus, which is connected to a buried power transmission coil, and the EV battery is charged

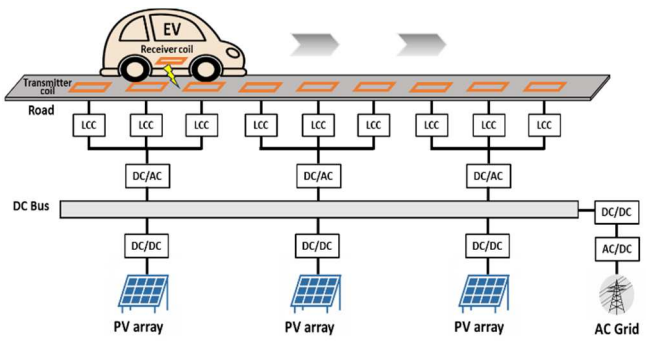

Fig.1 Overall picture of PV+DWPT system

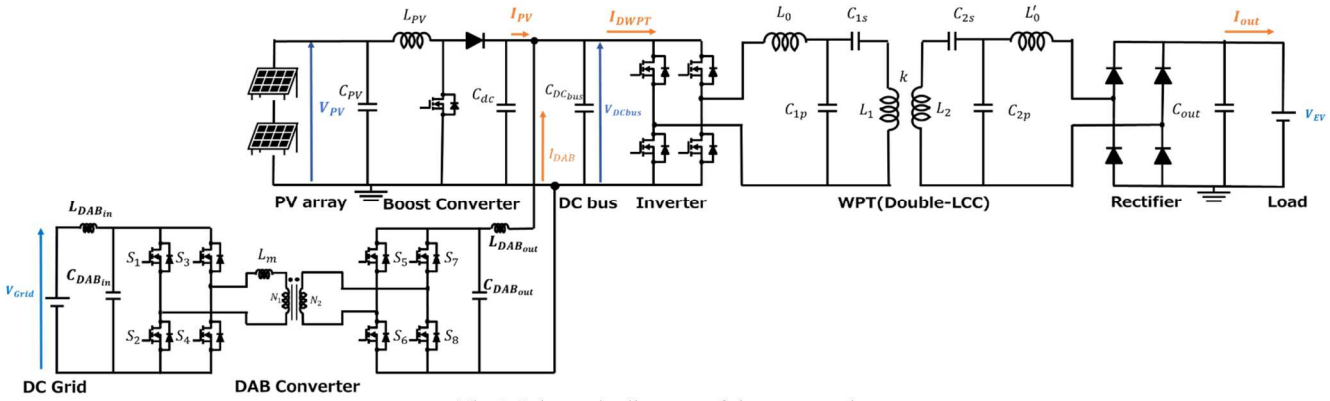

Fig.2 Schematic diagram of the proposed system

by the magnetic field coupling method when the EV equipped with the power receiving coil drives on the road.

Fig. 2 shows the circuit diagram of the entire system. From Fig. 2, many PV panels are installed near the road with power, and maximum power point tracking (MPPT) control is performed by a DC/DC boost converter operating at 10 kHz.

The DAB converter, which always obtains the maximum PV power, operates at 50 kHz in a square wave. By controlling the current output of the DAB converter, the DC bus is maintained at a constant level.

The DC/AC inverter connected to the DC bus performs switching at 85 kHz using a square wave. Finally, the Wireless Power Transfer (WPT) topology uses an LCC topology with the application of an LCL filter with gyrator characteristics to send power from the transmitting (roadside) coil to the receiving (vehicle side) coil to charge the battery of the EV.

In this study, the DC/DC boost converter on the EV side and the battery are simplified to a constant voltage source. Since the proposed system uses the same system configuration as in [8], we omit the description of each system.

B. Control Method of DAB Converter

DAB converters are frequently used as isolated bidirectional DC/DC converters to transform high voltages in power systems and for bidirectional power transmission [9]-[11]. The DAB converter is phase-shifted to control the voltage of the DC bus.

Fig. 3 shows the control block diagram of the DAB converter. In [8], the target value of the DC bus; $V_{DCbus_{ref}}$, is compared with the measured value; V_{DCbus}, referring to [11], and the phase shift is performed by determining the phase angle φ[rad] on the secondary side using PI control, which is feedback control, and feed-forward control was used to determine the phase angle φ[rad] of the secondary side using the target value $I_{DAB_{ref}}$ of the output current, and phase shift was performed.

In this paper, however, only feedback control is used to simplify the control. This control method enables the grids to adjust their power. The following equation shows how to obtain the phase angle φ. However, the direction sent from DCgrid to DC bus is the positive direction of $I_{DAB_{ref}}$.

$$\varphi \begin{cases} \dfrac{\pi}{2} - \dfrac{\pi}{2}\sqrt{1-\left(\dfrac{8f_{DAB}L_m I_{DAB_{ref}}}{n_t V_{grid}}\right)} & \left(I_{DAB_{ref}} > 0\right) \\ -\dfrac{\pi}{2} + \dfrac{\pi}{2}\sqrt{1-\left|\dfrac{8f_{DAB}L_m I_{DAB_{ref}}}{n_t V_{grid}}\right|} & \left(I_{DAB_{ref}} < 0\right) \end{cases}$$

III. METHOD

A. Simulation

The proposed system is simulated using circuit analysis software, based on the schematic diagram illustrated in Fig. 2.

A coupling coefficient k is set so that a vehicle equipped with one receiving coil runs at 12 km/h over a transmission coil with a laying ratio of 50%. The simulation demonstrates that the DC bus voltage remains steady, and the DWPT system operates stably, even with variations in the coupling coefficient between the transmitting and receiving coils.

Table 1 shows each parameter during the simulation. The parameters shown in (a) are those around the PV; the switching frequency of the DC/DC converter is designated as

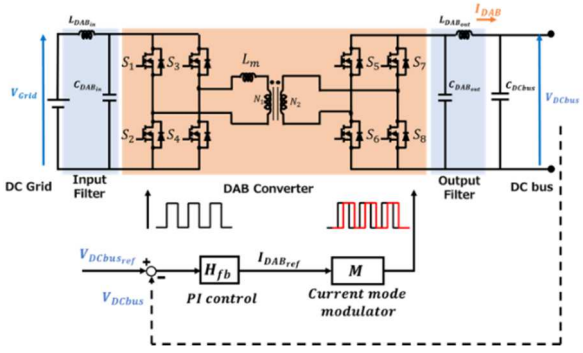

Fig.3 Block diagram of DAB converter control

Table 1. Simulation Parameters

(a) PV parameters

$f_{PV}[kHz]$	Δd	Duty sample	$L_{PV}[mH]$	$C_{PV}[\mu F]$	$C_{dc}[\mu F]$
10	0.01	0.01	0.1	500	100

(b) DAB parameters

$f_{DAB}[kHz]$	$V_{grid}[V]$	$V_{DCbus_{ref}}[V]$	n_t	$L_m[\mu H]$	$C_{DCbus}[\mu F]$
50	2400	600	4	50	500

(c) DWPT parameters

$f_{INV}[kHz]$	$L_0[\mu H]$	$C_{1p}[nF]$	$C_{1s}[nF]$	$L_1[\mu H]$	$L_0'[\mu H]$	$C_{2p}[nF]$	$C_{2s}[nF]$	$L_2[\mu H]$
85	54	65	23	207	49	71	56	111

f_{PV}, while the small variation in the duty cycle, adjusted using the mountain-climbing method for MPPT, is represented as Δd. The sampling time for updating the duty cycle is denoted as the Duty sample. The parameters related to the DAB converter are shown in (b), where f_{DAB} is the switching frequency, n_t is the transformer turn ratio, and V_{grid} and $V_{DCbus_{ref}}$ represent the DC grid voltage and the target DC bus voltage, respectively. In (c), the DWPT parameters are presented, with f_{INV} being the inverter's switching frequency and the resonant element values of the Double-LCC circuit specified.

The formulas for calculating the power for each parameter are the same as in [8] and are shown below.

$$P_{PV} = V_{PV} * I_{PV}$$
$$P_{grid} = V_{DCbus} * I_{DAB}$$
$$P_{in} = V_{DCbus} * I_{DWPT}$$
$$P_{out} = V_{out} * I_{out}$$

P_{PV} denotes the output power of the PV system, while P_{grid} represents the power corresponding to the positive direction of I_{DAB}, indicating power flow from the DC grid to the DC bus. P_{in} refers to the input power of the DWPT system, and P_{out} represents its output power of DWPT.

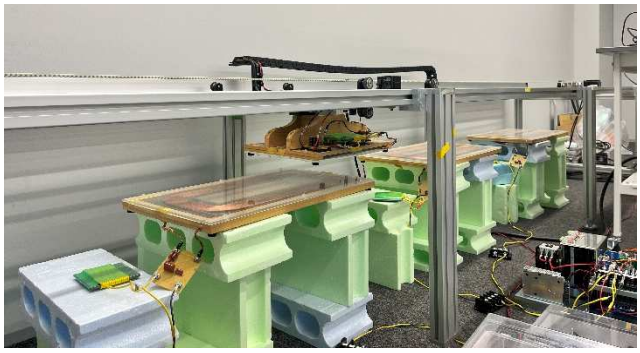

(a) Overall view of the experiment

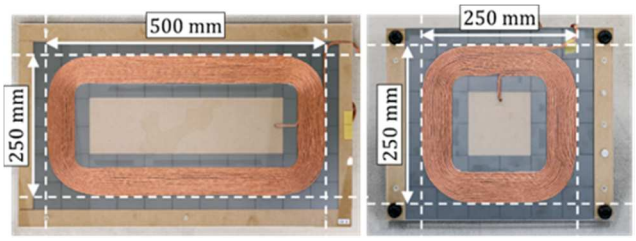

(b) Coils used in the experiment

Fig.4 Appearance of the bench-scale experiment

B. Bench-Scale Experiment

Based on the simulation methodology, bench-scale experiments will be conducted further to improve the proposed system's effectiveness and reliability.

Fig.4 and Fig.5 show the setup of the bench-scale experiment. In this experiment, a vehicle with one receiving coil (Rx) runs at 7 km/h over three transmission coils (Tx1~Tx3), is shown in Fig.4 (b). The size of all transmission coils is 500 mm x 250 mm, while the receiving coil is 250 mm x 250 mm. The air gap between the transmission and receiving coils is 80 mm.

Fig.5 shows the proposed system's overall view and how the bench-scale experiment is performed. The SAS (Solar Array Simulator) software can simulate the output characteristics of the PV panel and operate as if it were an actual PV panel system.

Table 2 shows the parameters for each device. The values around the DAB converter are shown in (a). The target value of the DC bus is set to 30V, which is 1/20 of the simulation value since high voltage cannot be handled due to the hardware limitation of the bench-scale experiment. The same values as in the simulation are used for the PV and DWPT parameters. (b) shows the parameters for each coil used in the experiment.

IV. RESULT

A. Simulation

Simulation results are shown in Figs. 6 and 7. Fig. 6 shows the coupling coefficient k of the DWPT and the results around the PV. (a) is the coupling coefficient from 0-2 seconds, and (b) is the amount of power generated from a PV irradiance of 1000 W/m2. In (c), the MPPT efficiency from the boost DC/DC converter is always 100%, indicating that the MPPT control worked properly.

Fig. 7 shows the results for the DAB converter and the DWPT. In (a), the variation of the DC bus voltage is shown.

Table 2. Experiment Parameters

(a) DAB parameters

$f_{DAB}[kHz]$	$V_{grid}[V]$	$V_{DCbus_{ref}}[V]$	n_t	$L_m[\mu H]$	$C_{DCbus}[\mu F]$
50	30	30	1	51.7	220

(b) WPT parameters

	Tx1	Tx2	Tx3	Rx
$L_0, L_0'[\mu H]$	53.6	49.8	49.6	49.2
$L_1, L_2[\mu H]$	206.9	206.7	206.4	111.4
$C_{1p}, C_{2p}[\mu F]$	65.4	70.4	70.8	71.2
$C_{1s}, C_{2s}[\mu F]$	22.9	22.3	22.3	56.4

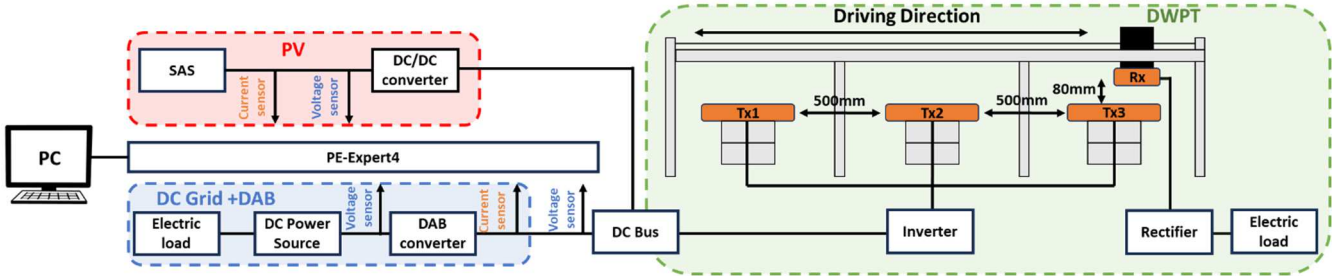

Fig.5 Overall view of the proposed system

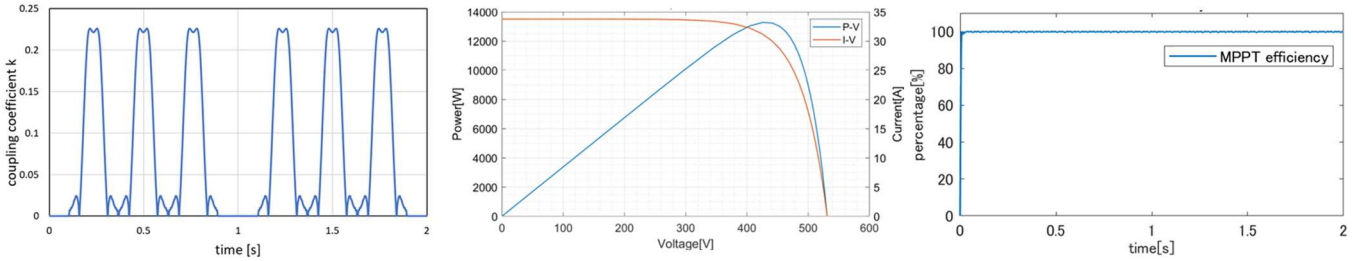

(a) Coupling coefficient k (b) P-V, I-V curve (c) MPPT efficiency

Fig.6 Coupling coefficient transition, P-V and I-V curve, results of MPPT.

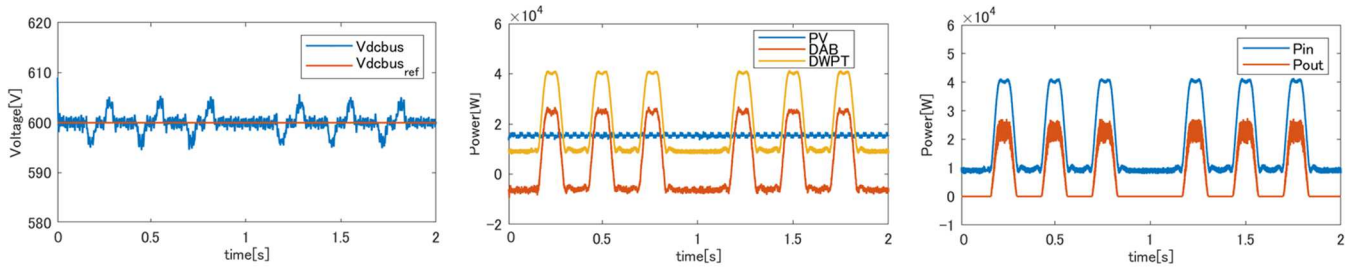

(a) V_{DCbus} against $V_{DCbusref}$ (b) Power of PV, DAB, DWPT (c) Input and output power of DWPT

Fig.7 Results of DAB current and PV, DAB, DWPT power.

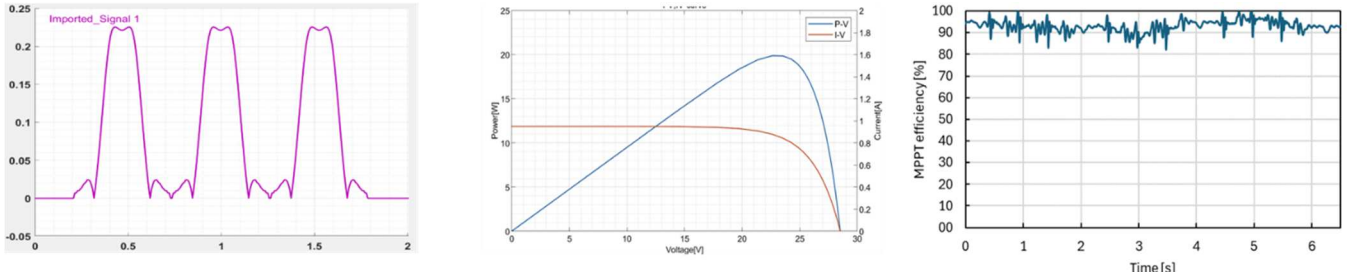

(a) Coupling coefficient k (b) P-V, I-V curve (c) MPPT efficiency

Fig.8 Coupling coefficient transition, P-V and I-V curve, results of MPPT.

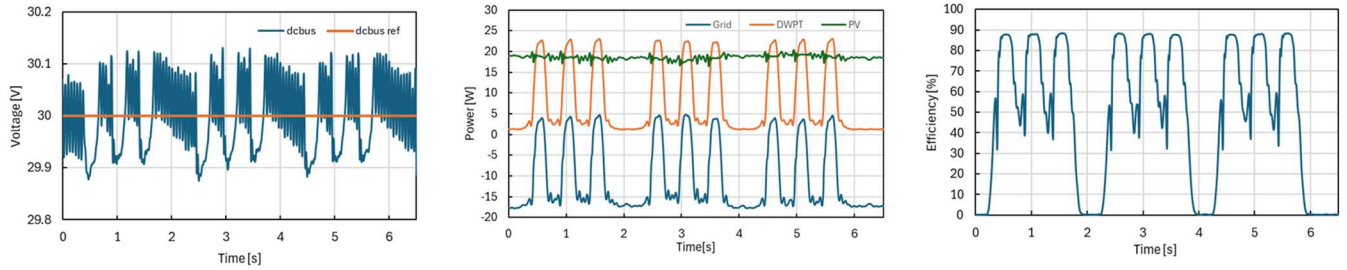

(a) V_{DCbus} against $V_{DCbusref}$ (b) Power of PV, DAB, DWPT (c) Power transmission efficiency

Fig.9 Results of DAB current and PV, DAB, DWPT power.

From the results, it can be read that V_{DCbus} is kept constant within ± 1% of the target value. Therefore, it can be said that constant voltage control of the DC bus was successfully performed. In (b), the variations of $P_{PV}, P_{grid}(= P_{DAB}), P_{DWPT}$ are shown. The results show that when there is no demand on the DWPT side, the PV power is sent to the DC grid. This indicates that DWPT is performing stably without wasting PV power. It can also be read that when the EV runs on the transmission coil, the DC grid supplies the amount of power that is not enough with just the PV power. Therefore, the DC grid helps maintain the power flow between the DWPT and the PV. In (c), P_{in} and P_{out} are shown. From the results, power is transmitted to the vehicle side as the coupling coefficient between the transmitting and receiving coils fluctuates. The maximum power transmission efficiency was about 70%. The reason for the relatively low

power transmission efficiency can be attributed to the simplification of the circuit on the EV side to a constant voltage source. Also, standby power is seen when the EV is not running on the transmission coil, but this may be because the connected inverter does not perform the switching control method which helps reduce standby loss.

B. Bench-Scale Experiment

The bench experiment results are shown in Figs. 8 and 9. In Fig. 8, (a), and (b), as in Fig. 6, we see that the coupling coefficient in (a) and the maximum PV power generation in (b) are 20W. In (c), the MPPT efficiency is always between 90% and 100%, indicating that the MPPT control is working properly.

Fig. 9 shows the results for the DAB converter and the DWPT section. In (a), the variation of the DC bus voltage is shown. From the results, it can be read that V_{DCbus} is kept constant within ±1% of the target value. Therefore, it can be said that constant voltage control was successfully performed. In (b), the power fluctuation of each system is shown. From the results, like the simulation results, power adjustment is performed based on the DWPT demand. The PV power oscillates a little just before the power transmission is performed, but we believe this is due to the small fluctuation of the voltage when the current control of DAB is performed to keep the DC bus voltage constant. (c) shows the power transmission efficiency, which is about 88%, indicating that power is being transmitted in a highly efficient and stable manner.

V. CONCLUSION

This paper proposes a PV+DWPT system that combines grid-connected PV and DWPT and demonstrates the system through simulations and bench experiments. The results showed that MPPT control of the PV was successfully performed while DWPT was used. Furthermore, the connected power system was able to absorb or supply the excess or deficiency of PV and keep the DC bus voltage constant, thus enabling stable DWPT. Conducting bench-scale experiments in addition to simulations further improved the effectiveness of the proposed PV+DWPT system and proved that it is a feasible system.

Based on the results of the simulation and the bench-scale experiment, we are planning to experiment on an actual vehicle to further verify the effectiveness of the proposed system. We will also work to further improve the effectiveness of control and power transmission efficiency when PV power generation fluctuates significantly.

REFERENCES

[1] C. Mi, G. Buja, S. Y. Choi, and C. T. Rim : “Modern Advances in Wireless Power Transfer Systems for Roadway Powered Electric Vehicles”, IEEE Transaction Industrial Electronics., Vol.63, No.10 pp.6533–6545 (2016)

[2] A. C. Bagchi, A. Kamineni, R. A. Zane and R. Carlson, "Review and Comparative Analysis of Topologies and Control Methods in Dynamic Wireless Charging of Electric Vehicles," in IEEE Journal of Emerging and Selected Topics in Power Electronics, vol. 9, no. 4, pp. 4947-4962, Aug. 2021.

[3] R. Tavakoli, T. Shabanian, E. M. Dede, C. Chou and Z. Pantic, "EV Misalignment Estimation in DWPT Systems Utilizing the Roadside Charging Pads," in IEEE Transactions on Transportation Electrification, vol. 8, no. 1, pp. 752-766, March 2022.

[4] A. N. Azad, A. Echols, V. A. Kulyukin, R. Zane and Z. Pantic, "Analysis, Optimization, and Demonstration of a Vehicular Detection System Intended for Dynamic Wireless Charging Applications," in IEEE Transactions on Transportation Electrification, vol. 5, no. 1, pp. 147-161, March 2019.

[5] K. Kumar, K. V. V. S. R. Chowdary, P. Sanjeevikumar, and R. Prasad, "Analysis of Solar PV Fed Dynamic Wireless Charging System for Electric Vehicles," *IECON 2021 – 47th Annual Conference of the IEEE Industrial Electronics Society*, Toronto, ON, Canada, 2021,

[6] S. Urano, M. Sugizaki, T. Imura, and Y. Hori, "Basic Experiment on the Integration of Grid-Connected Photovoltaic and Dynamic Wireless Power Transfer," *2022 IEEE 7th Southern Power Electronics Conference (SPEC)*, Nadi, Fiji, 2022, pp. 1-6,

[7] M. Sugizaki, S. Urano, T. Imura and Y. Hori, "Proposal for the System of Dynamic Wireless Power Transfer Connected with Photovoltaic in the Off-Grid Environment," *2022 IEEE 7th Southern Power Electronics Conference (SPEC)*, Nadi, Fiji, 2022, pp. 1-6

[8] N. Murayama, T. Imura and Y. Hori, "Power Stabilization of Dynamic Wireless Power Transfer System with Grid-connected Photovoltaic and DC Bus Voltage Control," *2024 IEEE Wireless Power Technology Conference and Expo (WPTCE)*, Kyoto, Japan, 2024, pp. 205-208

[9] P. Pal and R. K. Behera, "Observer-Based Current Sensorless Control for DAB Converter with Improved Dynamic Performance," *2022 IEEE International Conference on Power Electronics, Drives and Energy Systems (PEDES)*, Jaipur, India, 2022, pp. 1-6

[10] Y. -C. Jeung and D. -C. Lee, "Sliding mode control of bi-directional dual active bridge DC/DC converters for battery energy storage systems," *2017 IEEE Applied Power Electronics Conference and Exposition (APEC)*, Tampa, FL, USA, 2018

[11] Z. Shan, J. Jatskevich, H. H. -C. Iu and T. Fernando, "Simplified Load-Feedforward Control Design for Dual-Active-Bridge Converters With Current-Mode Modulation," in *IEEE Journal of Emerging and Selected Topics in Power Electronics*, vol. 6, no. 4, pp. 2073-2085, Dec. 2018